Prediction and Suppression of Twisted-wire Pair Crosstalk Based on Beetle Swarm Optimization Algorithm

Jianming Zhou [1], Shijin Li [1*], Wu Zhang [1], Wei Yan [1], Yang Zhao [1], Yanxing Ji [1], and Xingfa Liu [2]

[1] School of Electrical & Automation Engineering
Nanjing Normal University, Nanjing 210046, China
zhoujianmingz@163.com, *lishijin@njnu.edu.cn, m13571872250@163.com, 61197@njnu.edu.cn, zhaoyang2@njnu.edu.cn, 397832514@qq.com

[2] State Key Laboratory of Power Grid Environmental Protection
Wuhan Branch of China Electric Power Research Institute Co., Ltd., Wuhan 430000, China
liuxingfa@epri.sgcc.com.cn

Abstract ─ Based on the theory of multi-conductor transmission lines (MTL), this paper proposes a new method for predicting and suppressing crosstalk of twisted-wire pair (TWP). The per unit length (p.u.l) RLCG parameters change caused by the inconsistent cross-sectional shape of TWP, changes in parameters make it difficult to solve the telegraph equation. In this paper, the method of transmission lines cascade is used. TWP is divided into several segments, and p.u.l parameters of each segment are predicted. Compared with before method, we propose a higher precision algorithm—beetle swarm optimization (BSO) to optimize the weights of back-propagation (BP) neural network, which predict p.u.l parameters at each segment. On this basis, it is divided into two steps: 1) Use MTL frequency domain method combined with lines' terminal conditions to solve crosstalk and compare with CST simulation results; 2) Use the singular value decomposition (SVD) method to add matrix modules at both ends of lines for suppressing crosstalk. The results show that proposed method in this paper is consistent with the simulation, and the accuracy is higher than before.

Index Terms ─ Beetle swarm optimization, crosstalk, multi-conductor transmission lines, singular value decomposition.

I. INTRODUCTION

As people's requirements for electronic equipment increase, the circuit system gradually becomes smaller and more compact. The increase of the operating frequency has caused various electromagnetic interference (EMI) problems. Today, the effects of crosstalk between TWP cannot be ignored [1-3], then influence the signal integrity (SI). Unintentional coupling of energy between electro-magnetic fields will cause crosstalk in the line, in other words, the energy in the signal line is coupled to other lines. This part of the energy is useless [4]. The traditional MTL usually refers to a group of *n*-parallel conductor transmission line structures that propagate electrical signals in two or more fixed points. The crosstalk value can be achieved by directly solving the telegraph equation. However, the cross-section position in TWP is random and unknown, which brings different p.u.l RLCG parameters, so it is difficult to predict crosstalk directly by the traditional method [5,6].

In the past thirty years of research on crosstalk, many scholars have proposed a variety of TWP crosstalk prediction methods. Cannas proposed to treat non-uniformly TWP as cascade of several uniformly cross sections, and use BP neural network to make prediction [7]. In [8], Dai proposed to use the random displacement spline interpolation [9] (RDSI) to generate a set of non-uniformly TWP to provide training samples, and then use the trained BP to predict the crosstalk, but ordinary BP neural network have large errors, and its prediction range is narrow. In [10], the ANSI parameter matrix was proposed to predict the near-end crosstalk of unshielded TWP.

Based on the theory of MTL [11], some novel methods for suppressing crosstalk have been proposed. The proper feeding and matching modules at the line ends method was proposed in [12]. Increasing the effects of the capacitive coupling to cancel that of the inductive coupling along two parallel lines for reducing far end crosstalk is reported in [13]. By adding coefficient matrices at both ends of line, the unitization of transmission matrix is realized to suppress crosstalk have also been discussed [14]. However, these suppression methods are mainly aimed at parallel transmission lines,

Submitted On: November 10, 2020
Accepted On: January 28, 2021
https://doi.org/10.47037/2020.ACES.J.360409

and there is little research on TWP.

In fact, when the TWP is segmented, each fixed section position will correspond to a defined p.u.l matrix. This paper uses the cascade method [15] with BSO-BP algorithm, which has strong nonlinear mapping ability and is suitable for crosstalk prediction and suppression.

This paper is organized as follows. In Section II, MTL's distributed parameter circuit diagram and chain parameter theory will be given, the transmission lines model will be established. Besides, the process of BSO algorithm is introduced, the prediction errors of BSO, beetle antennae search (BAS) [16] and BP are compared in Section III. In Section IV, MTL frequency domain method will be used to solve the telegraph equation and be compared with the CST simulation results; the SVD method will be used to suppress crosstalk, and comparison figure before and after crosstalk suppression is given with PSPICE software. Conclusions are eventually drawn in Section V.

II. EQUIVALENT CIRCUIT AND CHAIN PARAMETER

A. Equivalent circuit

In MTL theory, the telegraph equation regards the transmission lines as having a distributed parameter structure along the axis. The micro-element conduction model of per unit length MTL is shown in Fig. 1. r_{ij}, l_{ij}, c_{ij} and g_{ij} represent the elements in resistance **R**, inductance **L**, capacitance **C**, and conductance **G** parameter matrices, where: i, j=1,2,…,n.

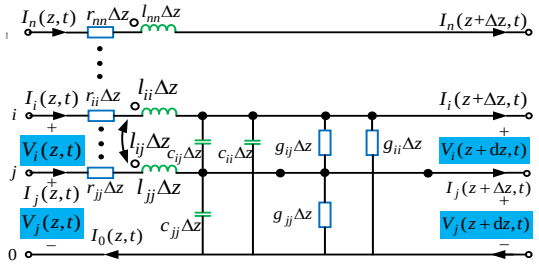

Fig. 1. The equivalent circuit model of micro-element.

The satisfied telegraph equations are expressed as:

$$\frac{\partial \mathbf{V}(z,t)}{\partial z}+\mathbf{R}(z)\mathbf{I}(z,t)+\mathbf{L}(z)\frac{\partial \mathbf{I}(z,t)}{\partial t}=0\,, \tag{1}$$

$$\frac{\partial \mathbf{I}(z,t)}{\partial z}+\mathbf{G}(z)\mathbf{V}(z,t)+\mathbf{C}(z)\frac{\partial \mathbf{V}(z,t)}{\partial t}=0\,, \tag{2}$$

where, $\mathbf{V}(z,t)$ and $\mathbf{I}(z,t)$ are voltage and current vectors at different positions and times on the transmission line. $\mathbf{R}(z)$, $\mathbf{L}(z)$, $\mathbf{C}(z)$, and $\mathbf{G}(z)$ are variables about the position z of transmission line, both of which are n-dimensional symmetric matrices.

B. Chain parameter

In this section, the transmission line will be regarded as a 2n port, and we generally care about the voltage and current at both ends of transmission line. First of all, convert equations (1) and (2) into frequency domain form:

$$\frac{d}{dz}\hat{\mathbf{V}}(z)=-\hat{\mathbf{Z}}\hat{\mathbf{I}}(z)\,, \tag{3}$$

$$\frac{d}{dz}\hat{\mathbf{I}}(z)=-\hat{\mathbf{Y}}\hat{\mathbf{V}}(z)\,, \tag{4}$$

where $\hat{\mathbf{Z}}=\mathbf{R}+j\omega\mathbf{L}$ and $\hat{\mathbf{Y}}=\mathbf{G}+j\omega\mathbf{C}$. Next the characteristic impedance matrix $\hat{\mathbf{Z}}_C$ of line is needed:

$$\hat{\mathbf{T}}_I^{-1}\hat{\mathbf{Y}}\hat{\mathbf{Z}}\hat{\mathbf{T}}_I=\hat{\boldsymbol{\gamma}}^2\,, \tag{5}$$

$$\hat{\mathbf{Z}}_C=\hat{\mathbf{Z}}\hat{\mathbf{T}}_I\boldsymbol{\gamma}^{-1}\hat{\mathbf{T}}_I^{-1}\,, \tag{6}$$

$$\hat{\mathbf{Y}}_C=\hat{\mathbf{Z}}_C^{-1}\,. \tag{7}$$

From [17], the relationship between the voltage and current at both ends of transmission line can be expressed by the chain parameter matrix:

$$\begin{bmatrix}\hat{\mathbf{V}}(\varphi)\\ \hat{\mathbf{I}}(\varphi)\end{bmatrix}=\hat{\Phi}(\varphi)\begin{bmatrix}\hat{\mathbf{V}}(0)\\ \hat{\mathbf{I}}(0)\end{bmatrix}=\begin{bmatrix}\hat{\Phi}_{11}(\varphi) & \hat{\Phi}_{12}(\varphi)\\ \hat{\Phi}_{21}(\varphi) & \hat{\Phi}_{22}(\varphi)\end{bmatrix}\begin{bmatrix}\hat{\mathbf{V}}(0)\\ \hat{\mathbf{I}}(0)\end{bmatrix}. \tag{8}$$

Where the sub-matrix can be defined as follows:

$$\hat{\Phi}_{11}(\varphi)=\cosh(\sqrt{\hat{\mathbf{Z}}\hat{\mathbf{Y}}}\varphi)\,, \tag{9}$$

$$\hat{\Phi}_{12}(\varphi)=-\hat{\mathbf{Z}}_C\sinh(\sqrt{\hat{\mathbf{Y}}\hat{\mathbf{Z}}}\varphi)\,, \tag{10}$$

$$\hat{\Phi}_{21}(\varphi)=-\hat{\mathbf{Y}}_C\sinh(\sqrt{\hat{\mathbf{Z}}\hat{\mathbf{Y}}}\varphi)\,, \tag{11}$$

$$\hat{\Phi}_{22}(\varphi)=\cosh(\sqrt{\hat{\mathbf{Y}}\hat{\mathbf{Z}}}\varphi)\,. \tag{12}$$

When the signal source amplitude is 1V, near-end crosstalk (NEXT) and far-end crosstalk (FEXT) are expressed as follows, i is the victim line number:

$$\mathrm{NEXT}_i=20*\log_{10}(V_i(0))\,, \tag{13}$$

$$\mathrm{FEXT}_i=20*\log_{10}(V_i(\varphi))\,. \tag{14}$$

III. BSO ALGORITHM

A. Modeling of TWP and single line

In this paper, the TWP and single line model in [18] are selected to verify the effectiveness of proposed method.

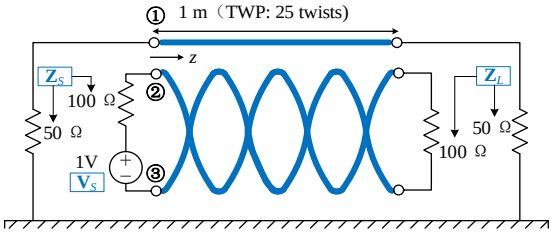

Fig. 2. Line configuration of a single line and TWP.

The model is shown in Fig. 2. Lines have a total

diameter d = 1.7 mm and a 0.11-mm thick PVC coating (relative permittivity of 2.7). The separation between the single line and the center of the TWP is s = 2.55 mm, so three lines are touching when they are lined up horizontally, and they lie at a height h = 5 cm above a perfect ground plane. Lines' length l= 1 m and TWP has N = 25 full twists (a lay length = 40 mm). Load at both ends of the transmission line: Z_S=Z_L=50Ω. The extracted p.u.l RLCG parameters and crosstalk are all based on this model.

B. BSO process introduction

Based on our previous research [19-21], we found that the optimization effect of BAS algorithm for high-dimensional data is not ideal, and its iterative results are greatly affected by initial position of the beetle. Therefore, inspired by the particle swarm algorithm, we have made improvements to the BAS algorithm based on expanded a single beetle into beetle group, which is the beetle swarm optimization (BSO) algorithm.

In this algorithm, each beetle represents a potential optimization solution. Similar to the particle swarm algorithm, beetles can share information with each other. However, the specific moving distance and direction of each beetle depends on the odor intensity it senses, which is the fitness function.

In this paper, we use BSO algorithm to optimize the weights of BP neural network. And on this basis, predict the p.u.l parameters at each segment position of TWP. The schematic diagram is shown in Fig. 3.

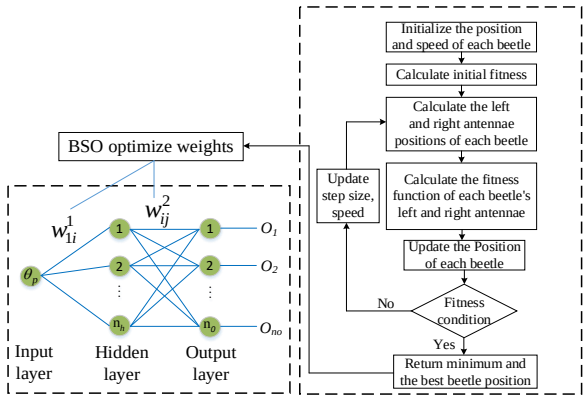

Fig. 3. BSO algorithm to optimize BP weights.

The number of hidden layers n_h is an empirical value determined by the number of input layers and output layers, which can be as follows:

$$n_h = \left(inputlayer + outputlayer\right)^{1/2} + a\,, \tag{15}$$

where a is the empirical constant between [1,10]. The hidden layer uses the sigmoid function $f(x)$, and output layer uses the linear function $g(x)$. They are as follows:

$$f\left(x\right) = \frac{1}{1+e^{-x}}\,, \tag{16}$$

$$g\left(x\right) = x\,. \tag{17}$$

Then, the output of neural network is:

$$y_j = \sum_{i=1}^{n_h} \frac{w_{ij}^2}{1+e^{-w_{1i}^1\theta_p}}\,. \tag{18}$$

For M sets of training samples, the mean square error E between the neural network output value y_j and the actual value $\hat{y}_j$ is:

$$E = \left(\frac{\sum_{j=1}^{M} (\hat{y}_j - y_j)^2}{M} \right)^{1/2}\,. \tag{19}$$

Next, the specific steps of BSO algorithm to optimize weights w_{1i}^1 and w_{ij}^2 will be introduced. Here, the position of each beetle is the BP weight, and the fitness function is the BP neural network error E.

Step 1: Generate a group of n beetles: $B = (B_1, B_2, \cdots B_n)$ in an S-dimensional search space, where the i th beetle represents a vector: $B_i = (b_{i1}, b_{i2}, \cdots b_{iS})$, this represents a potential solution to the optimization problem. The speed of the i th is expressed as: $V_i = (V_{i1}, V_{i2}, \cdots V_{iS})$. In order to improve the calculation speed, we have stipulated the threshold range for the individual and the whole beetle: $U_i = (U_{i1}, U_{i2}, \cdots U_{iS})$ and $U_g = (U_{g1}, U_{g2}, \cdots U_{gS})$.

Step 2: Give the iterative formula of beetle position B_{is}^{k+1} and speed V_{is}^{k+1}.

$$B_{is}^{k+1} = B_{is}^{k} + \lambda V_{is}^{k} + (1-\lambda)\delta_{is}^{k}\,, \tag{20}$$

where s=1,2,…S; i=1,2,…n; k is the current number of iterations. δ_{is} is increase in beetle position movement. λ is a constant.

$$V_{is}^{k+1} = \omega V_{is}^{k} + c_1 r_1 (U_{is}^{k} - B_{is}^{k}) + c_2 r_2 (U_{gs}^{k} - B_{gs}^{k})\,, \tag{21}$$

where ω is inertia weight, c_1, c_2 are constants, r_1 and r_2 are two random functions in the range [0,1].

Step 3: Give the distance and direction of the beetle.

$$\delta_{is}^{k+1} = \varepsilon^{k} * V_{is}^{k} * sign(f(B_{rs}^{k}) - f(B_{ls}^{k}))\,. \tag{22}$$

In this step, ε is step size. The search functions of the left and right antennae of beetle are respectively expressed as:

$$B_{rs}^{k+1} = B_{rs}^{k} + V_{is}^{k} * d/2\,, \tag{23}$$

$$B_{ls}^{k+1} = B_{ls}^{k} - V_{is}^{k} * d/2\,, \tag{24}$$

d represents the distance between two antennae. After the iterative loop is over, return a minimum error value, and the corresponding beetle position, that is, the weights.

C. Error comparison

In this section, we use ANSYS software to extract a set of p.u.l parameters at fixed rotation degrees (0: 5: 175 degrees) as training samples first. Secondly, rotation degrees θ_p are used as the neural network input, and p.u.l RLCG parameters is combined into one column as the output **O**.

$$\mathbf{O} = [tri(\mathbf{R}), tri(\mathbf{L}), tri(\mathbf{C}), tri(\mathbf{G})]^T . \quad (25)$$

Then use BP neural network optimized by BSO and BAS to predict p.u.l. RLCG parameters. In Fig. 4, iterative fitness (error) of BSO and BAS are compared.

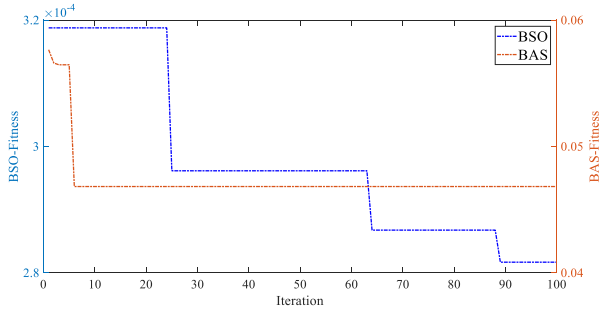

Fig. 4. BSO and BAS iteration error comparison.

It can be inferred from Fig. 4 that compared to BAS, the group optimization method used by BSO reduces the iteration error by 187.5 times, and it is almost unaffected by the initial position of beetle. We use trained neural network to predict the original training samples again and compare two samples' error. Taking **L** parameter matrix elements l_{ij} as example, the relative prediction error under three algorithms of BS0-BP, BAS-BP and BP are given.

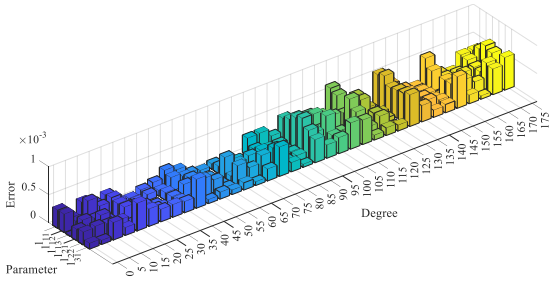

(a)

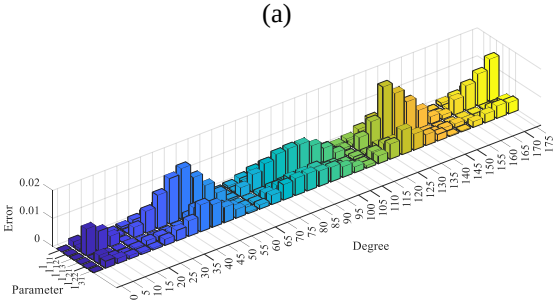

(b)

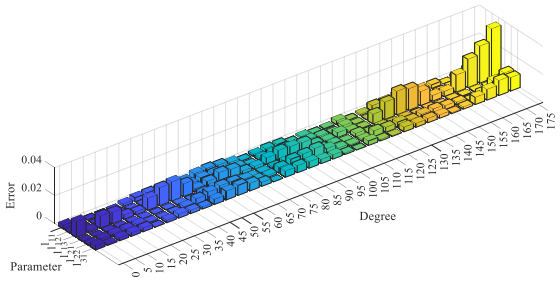

(c)

Fig. 5. BSO-BP, BAS-BP and BP prediction error comparison (a) BSO-BP, (b) BAS-BP, and (c) BP.

It can be seen from Fig. 5 that compared with the previous BAS and BP algorithms, the prediction accuracy of BSO for parameters has been improved by more than 20 times.

IV. CROSSTALK PREDICTION AND SUPPRESSION VERIFICATION

A. MTL frequency domain method to solve crosstalk

After the p.u.l parameters at each segment have been obtained, the MTL frequency domain method combined with terminal conditions is used to solve crosstalk. In the Section II, we have derived the chain parameter expression of transmission line. Then crosstalk solutions based on the terminal condition are given.

From equation (8):

$$[\hat{\Phi}_{12} - \hat{\Phi}_{11}\hat{\mathbf{Z}}_S - \hat{\mathbf{Z}}_L\hat{\Phi}_{22} + \hat{\mathbf{Z}}_L\hat{\Phi}_{21}\hat{\mathbf{Z}}_S]\hat{\mathbf{I}}(0) = [\hat{\mathbf{Z}}_L\hat{\Phi}_{21} - \hat{\Phi}_{11}]\hat{\mathbf{V}}_S , \quad (26)$$

$$\hat{\mathbf{I}}(\varphi) = \hat{\Phi}_{21}\hat{\mathbf{Z}}_S + [\hat{\Phi}_{22} - \hat{\Phi}_{21}\hat{\mathbf{Z}}_S]\hat{\mathbf{I}}(0), \quad (27)$$

where $\hat{\mathbf{Z}}_S$ and $\hat{\mathbf{Z}}_L$ are termination load matrix. $\hat{\mathbf{V}}_S$ is the power supply.

Combined with terminal conditions:

$$\hat{\mathbf{V}}(0) = \hat{\mathbf{V}}_S - \hat{\mathbf{Z}}_S\hat{\mathbf{I}}(0), \quad (28)$$

$$\hat{\mathbf{V}}(\varphi) = \hat{\mathbf{Z}}_L\hat{\mathbf{I}}(\varphi). \quad (29)$$

The 2*n* terminal voltages $\hat{\mathbf{V}}(0)$ and $\hat{\mathbf{V}}(\varphi)$ can be obtained from equations (26-29).

Next, compare crosstalk obtained based on the three parameter prediction methods with the CST simulation software results, as shown in Fig. 5. The frequency range of crosstalk result is 5MHz ~ 1GHz.

In Fig. 6, the optimized algorithm can maintain good consistency with the results in CST. And compared with BAS, it is obvious that BSO has better fit and high accuracy. Next, we provide the relative error of predicting crosstalk in three methods under sub-frequency band and sub-port in Table 1.

Among them, the highest error is BP, and the lowest is BSO-BP, which also reflects the necessity of optimization algorithm. The FEXT prediction accuracy

is better than NEXT. In the sub-frequency bands: prediction accuracy for low frequency band is the highest, and the accuracy is the lowest in the mid frequency band due to large number of resonance points.

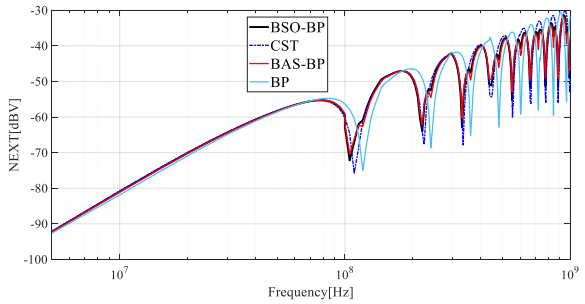

(a)

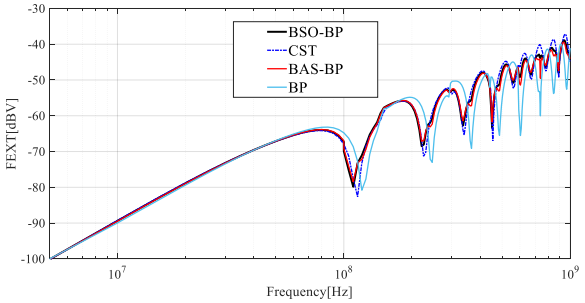

(b)

Fig. 6. Comparison of crosstalk under three parameter prediction algorithms (a) NEXT and (b) FEXT.

Table 1: Average error (%) of crosstalk prediction (N: NEXT; F: FEXT)

Frequency (MHz)	**5~100**		**100~500**		**500~1000**	
	N	F	N	F	N	F
BSO-BP	2.32	2.23	19.19	15.76	21.94	8.35
BAS-BP	5.71	5.47	40.00	35.65	43.45	21.44
BP	13.53	13.72	92.75	88.93	95.31	67.96

B. SVD method to suppress crosstalk

Based on equations (8-12), we can obtain the relationship between the far-end and near-end voltages of the transmission line, defined as **P**:

$$\begin{aligned}\hat{\mathbf{V}}(\varphi) &= \mathbf{P}\hat{\mathbf{V}}(0) \\ &= [\hat{\Phi}_{11}(\varphi)+\hat{\Phi}_{12}(\varphi)(\hat{\Phi}_{12}(\varphi)-\mathbf{Z}_L\hat{\Phi}_{22}(\varphi))^{-1} \\ &\quad \cdot(\hat{\Phi}_{11}(\varphi)-\mathbf{Z}_L\hat{\Phi}_{21}(\varphi))]\hat{\mathbf{V}}(0). \end{aligned} \quad (30)$$

The non-diagonal elements in the matrix **P** correspond to crosstalk. If the matrix **P** is transformed into a unit matrix, the crosstalk is suppressed. We can use singular value decomposition (SVD) in matrix theory to achieve this goal. For the P matrix, since it is a full rank ($n\times n$) matrix, there are unitary matrices **G** and **F** exist, such that:

$$\mathbf{G}^H\mathbf{P}\mathbf{F}=\mathbf{B}, \quad (31)$$

where **B** is the diagonal matrix, σ is the singular value of **P**, and then:

$$\mathbf{P}=\mathbf{G}\mathbf{B}\mathbf{F}^H, \quad (32)$$

$$\mathbf{G}^H\mathbf{P}\mathbf{F}\mathbf{B}^{-1}=\mathbf{E}_n. \quad (33)$$

From (32), it can be seen that the transmission matrix **P** become an identity matrix, which needs to undergo three signal transformations:

1) The first signal transformation occurs at the input of the transmission line: $\mathbf{B}^{-1}$.

2) The second signal transformation occurs after the first transformation: **F**.

3) The third signal transformation occurs at the output of the transmission line: $\mathbf{G}^H$.

We define:

$$\mathbf{P}_b=\mathbf{F}\mathbf{B}^{-1}, \quad (34)$$

$$\mathbf{P}_e=\mathbf{G}^H. \quad (35)$$

In other words, the crosstalk can be suppressed by implementing two matrix operations at the transmission line ends. The crosstalk suppression circuit $\mathbf{P}_b$ on the source end is shown in Fig. 7, and the load end $\mathbf{P}_e$ is also the same implementation circuit.

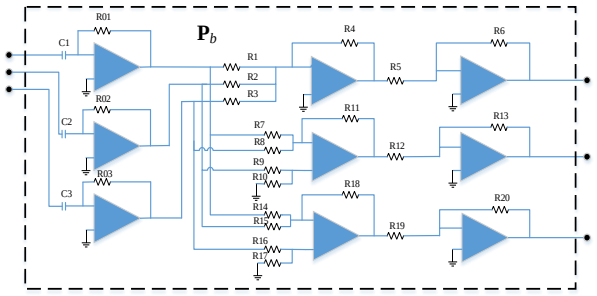

Fig. 7. Crosstalk suppression circuit.

We select operational amplifiers as the components for matrix operation, and negative feedback circuits formed by operational amplifier can meet requirements. Then, simulations are performed before and after crosstalk suppression in PSPICE. Because at high frequencies, $\omega\mathbf{L}>>\mathbf{R}$ and $\omega\mathbf{C}>>\mathbf{G}$, therefore in this part: **R=G=0**.

Due to the unidirectional conductivity of the operational amplifier, NEXT will not exist. Next, we give the FEXT suppression effect under 100MHz sinusoidal signal.

It can be seen from Fig. 8 that suppress crosstalk method proposed in this paper is effective, and its effect partly depends on the accuracy of circuit components.

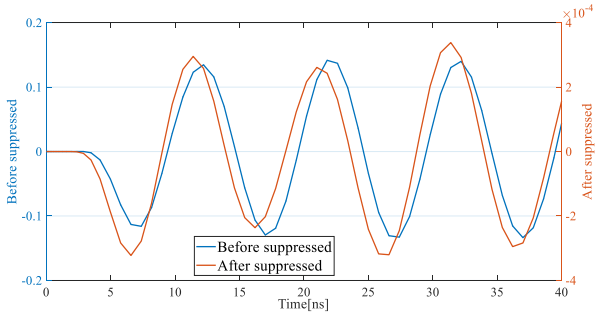

Fig. 8. FEXT suppression effect comparison.

V. CONCLUSION

In this paper, a new algorithm for predicting the p.u.l RLCG parameters of TWP is proposed: beetle swarm optimization. Based on the transmission lines cascade theory, the TWP is divided into several segments, each segment is regarded as a parallel transmission line, and crosstalk is solved and suppressed through the p.u.l parameter.

In this paper, the newly proposed BSO algorithm is compared with the previous BAS and BP algorithms, which proves that BSO has smaller iteration errors and better convergence, so that the accuracy of parameter prediction is higher.

The verification in Section IV is divided into two parts, namely solving and suppressing crosstalk. In the first part, using the MTL frequency domain analysis method to solve crosstalk is given, and three prediction methods are compared with the CST results to prove the improvement of BSO; the second part uses the SVD method to add auxiliary circuit at both ends of the transmission line, which composed of operational amplifiers. Its purpose is to turn the transmission matrix into a unit matrix. Finally, the comparison figure before and after crosstalk suppression is given with the PSPICE software.

ACKNOWLEDGMENT

This work is supported by the National Natural Science Foundation of China under Grant (51475246), the National Natural Science Foundation of Jiangsu Province under Grant (BK20161019), the Aviation Science Foundation under Grant (20172552017), the Key Project of Social Development in Jiangsu Province under Grant (BE2019716), the Open Fund Project of State Key Laboratory of Power Grid Environmental Protection under Grant (GYW51202001558), and the Nanjing International Industrial Technology Research and Development Cooperation Project under Grant (201911021).

REFERENCES

[1] S. Chabane, P. Besnier, and M. Klingler, "A modified enhanced transmission line theory applied to multiconductor transmission lines," *IEEE Trans. Electromagn. Compat.*, vol. 59, no. 2, pp. 518-528, Apr. 2017.

[2] F. Grassi and S. A. Pignari, "Immunity to conducted noise of data transmission along DC power lines involving twisted-wire pairs above ground," *IEEE Trans. Electromagn. Compat.*, vol. 55, no. 1, pp. 195-207, Feb. 2013.

[3] Y. Guo, L. Wang, and C. Liao, "Crosstalk spectrum predictions considering frequency-dependent parameters in electric vehicles," *Applied Computational Electromagnetics Society Journal*, vol. 30, no. 5, pp. 551-557, May 2015.

[4] J. L. Rotgerink, H. Schippers, and F. Leferink, "Low-Frequency analysis of multiconductor transmission lines for crosstalk design rules," *IEEE Trans. Electromagn. Compat.*, vol. 61, no. 5, pp. 1612-1620, Oct. 2017.

[5] G. Spadacini, and S. A. Pignari, "Numerical assessment of radiated susceptibility of twisted-wire pairs with random non-uniform twisting," *IEEE Trans. Electromagn. Compat.*, vol. 55, no. 5, pp. 956-964, Jan. 2013.

[6] G. Spadacini and S. A. Pignari, "Radiated susceptibility of a twisted-wire pair illuminated by a random plane-wave spectrum," *IEICE Trans. Commun.*, vol. E93-B, no. 7, pp. 1781-1787, July 2010.

[7] B. Cannas, A. Fanni, and F. Maradei, "A neural network approach to predict the crosstalk in non-uniform multiconductor transmission lines," *IEEE International Symposium on Circuits and Systems. Proceedings (Cat. No.02CH37353)*, Phoenix-Scottsdale, pp. 573-576, 2002.

[8] F. Dai, G. H. Bao, and D. L. Su, "Crosstalk prediction in non-uniform cable bundles based on neural network," *Proceedings of the 9th International Symposium on Antennas, Propagation and EM Theory*, Guangzhou, pp. 1043-1046, 2010.

[9] S. Sun, G. Liu, J. L. Drewniak, and D. J. Pommerenke, "Hand-assembled cable bundle modeling for crosstalk and common-mode radiation prediction," *IEEE Trans. Electromagn. Compat.*, vol. 49, no. 3, pp. 708-718, Aug. 2007.

[10] O. Olusegun, A. Duffy, and C. Nche, "Parameter for near end crosstalk prediction in twisted pair cables," *2016 IEEE International Symposium on Electromagnetic Compatibility (EMC)*, Ottawa, pp. 485-490, 2016.

[11] D. F. Wiliams, L. A. Hayden, and R. B. Marks, "A complete multimode equivalent-circuit theory for electrical design," *Journal of Research of the National Institute of Standards and Technology*, vol. 102, no. 4, pp. 405-423, Aug. 1997.

[12] T. Ciamulski and W. K. Gwarek, "A study of feeding options aimed at canceling crosstalk in

multiconductor transmission lines," *IEEE MTT-S International Microwave Symposium Digest, (IEEE Cat. No.04CH37535)*, Fort Worth, pp. 1631-1634, 2004.

[13] M. H. Wu, W. J. Chen, J. W. Liang and X. B. Fang, "An improvement method of the increasing mutual capacitance for reducing far-end crosstalk in transmission line," *IEEE Antennas and Propagation Society International Symposium*, Albuquerque, pp. 1227-1230, 2006.

[14] V. Vladimir and R. Ianconescu, "Transmission of the maximum number of signals through a multiconductor transmission line without crosstalk or return loss: Theory and simulation," *IET Microwaves, Antennas & Propagation*, vol. 9, no. 13, pp. 1444-1452, Oct. 2015.

[15] A. Shoory, M. Rubinstein, A. Rubinstein, C. Romero, N. Mora, and F. Rachidi, "Application of the cascaded transmission line theory of Paul and McKnight to the evaluation of NEXT and FEXT in twisted wire pair bundles," *IEEE Trans. Electromagn. Compat.*, vol. 55, no. 4, pp. 648-656, Aug. 2013.

[16] Z. Zhu, Z. Zhang, W. Man, X. Tong, J. Qiu, and F. Li, "A new beetle antennae search algorithm for multi-objective energy management in microgrid," *2018 13th IEEE Conference on Industrial Electronics and Applications (ICIEA)*, Wuhan, pp. 1599-1603, 2018.

[17] C. R. Paul, *Analysis of Multiconductor Transmission Lines*. 2nd ed., New York, USA: Wiley, 1994.

[18] P. Manfredi, D. D. Zutter, and D. V. Ginste, "Analysis of nonuniform transmission lines with an iterative and adaptive perturbation technique," *IEEE Trans. Electromagn. Compat.*, vol. 58, no. 3, pp. 859-867, June 2016.

[19] C. P. Yang, W. Yan, Y. Zhao, Y. Chen, C. M. Zhu, and Z. B. Zhu, "Analysis on RLCG parameter matrix extraction for multi-core twisted cable based on back propagation neural network algorithm," *IEEE Access*, vol. 7, pp. 126315-126322, Aug. 2019.

[20] C. Huang, W. Yan, Y. Zhao, Q. Q. Liu, and J. M. Zhou, "A new method for predicting crosstalk of random cable bundle based on BAS-BP neural network algorithm," *IEEE Access*, vol. 8, pp. 20224-20232, Jan. 2020.

[21] Q. Q. Liu, Y Zhao, W Yan, C Huang, M. Abdul, and Z Meng, "A novel crosstalk estimation method for twist non-uniformity in twisted-wire pairs," *IEEE Access*, vol. 8, pp. 38318-38326, Feb. 2020.